Measurement of Signal Velocity in a Region of Resonant Absorption by Ultrasonic Paramagnetic Resonance

N. S. SHIREN*
General Electric Research Laboratory, Schenectady, New York
(Received June 4, 1962)

Measurements of signal velocity for wave propagation at frequencies within a narrow absorption band are reported. The measurements were made on pulsed microwave ultrasonic waves propagating in single crystal MgO and interacting with paramagnetic resonance absorption lines of Ni^{2+} and Fe^{2+} impurity ions, present in low concentrations. The lines are inhomogeneously broadened, and a comparison of observed velocities with theory then requires knowledge of homogeneous spin packet linewidths. These are estimated from the theory of dipolar broadening. The experimental results are found to lie within theoretical limits established by calculations of Brillouin and Baerwald, provided that the spatial scale of the random magnetic inhomogeneities, which cause inhomogeneous line broadening, is assumed large compared with the acoustic wavelength. If this assumption is not made, the observed changes in signal velocity were larger than theory predicts by as much as three orders of magnitude. Thus, as byproducts of these experiments, it is found that ultrasonic velocity measurements may be used to estimate the scale of inhomogeneities, and also to measure spin packet linewidths in the presence of inhomogeneous broadening.

I. INTRODUCTION

THE problem of wave propagation within or near a narrow absorption band (and, therefore, in a region of strong anomalous dispersion) was first considered by Laue[1] and then by Sommerfeld.[2] Its importance lay in an apparent contradiction with the theory of relativity; the group velocity, which is the velocity of energy flow in nondissipative media, becomes larger than c within an absorption band. The problem and some of the theoretical results are quoted in several textbooks on optics and electromagnetic theory,[3] and a review has been published recently by Brillouin.[4] However, no quantitative experimental measurements, leading to a comparison with the theories, have been reported.

It is difficult to define a propagation velocity for signals having frequencies within an absorption band because of the resulting distortion of the signal shape. However, Sommerfeld[5] showed quite generally that no part of the signal may travel at a velocity greater than c. Brillouin[6] extended these calculations, and using a certain mathematical definition of signal velocity, computed this velocity as a function of frequency through the absorption band. Using a more exact method of integration, Baerwald[7] showed that the observed signal velocity will depend on the length of the propagation path, and calculated an asymptotic signal velocity valid for large path lengths.

Although the original problem was concerned with light propagation, the arguments are nonrelativistic and apply equally well to any plane wave propagation in a continuum, provided c is taken to mean the characteristic velocity of the transmission medium in the absence of absorbers.

In this paper, we report the results of what appears to be the first measurement of signal velocity in a medium containing narrow resonance absorption lines. The measurements were made using pulsed microwave ultrasonic waves propagating in single crystal MgO. The interaction of the ultrasonics with paramagnetic resonances of Ni^{2+} and Fe^{2+} impurity ions provided the absorption lines. When the ultrasonic frequency is near one of the resonances, those pulses which have traversed the MgO crystal exhibit later arrival times than when the frequency is off resonance, thus, indicating a decrease in the signal velocity. An example is shown in Fig. 1, where the second pulse in each trace has made one round trip through the MgO.

In Sec. II we review the theoretical results and modify them to apply to acoustic paramagnetic resonance with inhomogeneous line broadening, and also to ultrasonic wave propagation in a medium with a randomly distributed refractive index. In Sec. III the experimental technique is presented, and some pertinent aspects of paramagnetic resonance are discussed briefly. The experimental data are presented in Sec. IV.

In Sec. V it is shown that the experiments confirm the theoretical results of Brillouin and Baerwald, and this is the principal result reported. However, it is also found that ultrasonic velocity measurements provide a technique for measuring the dimensional scale of magnetic

* Present address: IBM, Thomas J. Watson Research Center, Yorktown Heights, New York. Most of the analysis and theory were done at this location.

[1] M. Laue, Ann. Physik **18**, 523 (1905).

[2] A. Sommerfeld, Physik Z. **8**, 841 (1907).

[3] See, for example, A. Sommerfeld, *Optics* (Academic Press Inc., New York, 1954), Chap. 2, pp. 114–128; F. A. Jenkins and H. E. White, *Fundamentals of Physical Optics* (McGraw-Hill Book Company, Inc., New York, 1937), 1st ed., Chap. 2, p. 301; J. A. Stratton, *Electromagnetic Theory*, (McGraw-Hill Book Company, Inc., New York, 1941), 1st ed., Chap. 5, pp. 333–340; W. K. H. Panofsky and M. Phillips, *Classical Electricity and Magnetism* (Addison-Wesley Publishing Company, Inc., Cambridge, Mass. 1955), 1st ed., Chap. 21, pp. 330–332.

[4] L. Brillouin, *Wave Propagation and Group Velocity* (Academic Press Inc., New York, 1960).

[5] A. Sommerfeld, Ann. Physik **44**, 177 (1914).

[6] L. Brillouin, Ann. Physik **44**, 203 (1914).

[7] H. Baerwald, Ann. Physik **7**, 731 (1930).

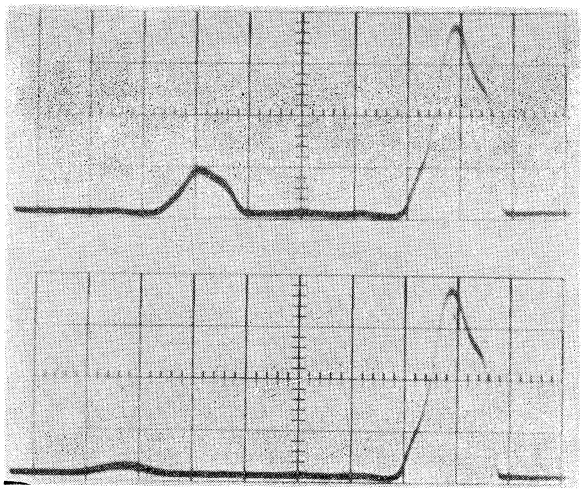

FIG. 1. Oscilloscope traces showing change in ultrasonic signal velocity due to interaction with Fe^{2+} spin resonance in MgO. Time increases from right to left. The first pulse is a bond echo and has traveled through the quartz transducer only. The second pulse has made one round trip in the MgO. Upper trace: ultrasonic frequency off resonance. Lower trace: ultrasonic frequency on resonance.

inhomogeneities, and for the determination of homogeneous linewidths in the presence of inhomogeneous broadening.

We have also included an Appendix on the calculation of dipolar broadening of ultrasonically induced spin resonance transitions in magnetically dilute systems.

II. THEORY

Review

The mathematical methods used in the calculation of signal velocity have been reviewed by Brillouin.[4] The input signal is taken to be the step-function sine wave,

$$f(t)=0, \quad t\leq 0,$$
$$f(t)=\sin\omega t, \quad t>0. \tag{1}$$

This function may be defined by a Fourier integral in the complex $\bar{\omega}$ plane;

$$f(t)=\lim_{\epsilon\to 0}\frac{1}{2\pi}\,\mathrm{Re}\int_{-\infty}^{+\infty}\frac{\exp(-i\bar{\omega}t)}{\bar{\omega}-(\omega-i\epsilon)}d\bar{\omega}, \tag{2}$$

with the contour taken along the real axis from $-\infty$ to $+\infty$, passing above the pole. For $t<0$ the contour is closed at $|\bar{\omega}|=\infty$ in the upper half plane, and for $t>0$ at $|\bar{\omega}|=\infty$ in the lower half-plane. The solution of the one-dimensional wave equation for a plane wave propagating in the positive x direction with $f(t)$ as input at $x=0$ is then

$$F(t,x)=\lim_{\epsilon\to 0}\frac{1}{2\pi}\,\mathrm{Re}\int_{-\infty}^{+\infty}\frac{\exp\{i[-\bar{\omega}t+k(\bar{\omega})x]\}}{\bar{\omega}-(\omega-i\epsilon)}d\bar{\omega}; \tag{3}$$

$$F(t,0)=f(t).$$

The model taken for the propagation medium is a gas consisting of a uniform distribution of Lorentz oscillators with resonant frequency ω_0. Then,

$$k^2(\omega)=[\alpha(\omega)+i\beta(\omega)]^2=\frac{\omega^2}{c^2}\left(1+\frac{a^2}{\omega_0^2-\omega^2-2i\omega\delta}\right), \tag{4}$$

where c is the characteristic velocity (at $\omega=\infty$) of the medium, including all nondissipative terms, a^2 is proportional to the interaction strength and to the oscillator density, and δ is the oscillator damping. The phase velocity of a stationary wave at frequency ω is $[\omega/\alpha(\omega)]$, and its differential damping is $\beta(\omega)$. The integrand of Eq. (3) has branch points in the lower half-plane [at the poles and zeros of $k(\bar{\omega})$, and the contour must be appropriately deformed from that used in evaluating Eq. (1)].

The propagation of a signal at frequency ω, within the absorption band, is characterized by a set of low level forerunners which precede the arrival of the main body of the signal, and consist principally of frequency components which lie both above and below the absorption band. The amplitude of the forerunners gradually decays as the stationary component, of frequency ω, builds up to its final value

$$F(t,x)=e^{-\beta(\omega)x}\sin[\omega t-\alpha(\omega)x]. \tag{5}$$

Due to the resulting distortion of the signal shape the definitions of signal velocity are somewhat arbitrary. Both Brillouin's and Baerwald's definitions are expressed in terms of the formalisms used in evaluating the integral of Eq. (3), and their physical equivalence is only approximate. Thus, within their regions of validity (discussed below) both definitions correspond, physically, to defining the signal arrival time as the time at which the stationary amplitude reaches some fraction of its final value. However, the measured change in arrival time (from x/c) will be practically independent of the actual fractional amplitude used, as long as the latter is very much larger than the forerunner amplitude.

According to Baerwald's theory there is a critical depth of propagation, x_{crit}, beyond which the calculation of Brillouin is invalid. This depth is also expressed in terms of the mathematical formalism, but is approximately given by

$$x_{\mathrm{crit}}\approx 5.3\left\{\left|\frac{d^2k(\omega)}{d\omega^2}\right|\Big/\left(\frac{dk_i(\omega)}{d\omega}\right)^2\right\}_{\omega}, \tag{6}$$

where $k_i(\omega)$ is the imaginary part of $k(\omega)$. Using Eq. (4), under the conditions of interest in this paper,

$$\delta/\omega_0\ll 1, \quad a^2/4\omega_0\delta\ll 1, \tag{7}$$

we find

$$x_{\mathrm{crit}}\approx 1/\beta(\omega). \tag{8}$$

For propagation distances very much larger than x_{crit}, the reciprocal of the signal velocity, $S(\omega)^{-1}$, approaches

the asymptotic value calculated by Baerwald,

$$[S_A(\omega)]^{-1}=[\beta(\omega)/\delta]+1/c. \tag{9}$$

$[S(\omega)]^{-1}$ decreases with decreasing x and approaches the value computed by Brillouin when $x\ll x_{\text{crit}}$.

A velocity of energy flow may be defined as the energy flux divided by the energy density. In nondissipative media this velocity is equal to the group velocity, $d\omega/dk$.[8] However, in the case of resonant absorption the energy velocity is equal to the asymptotic signal velocity, $S_A(\omega)$, in the region $\omega\approx\omega_0$, provided also that the conditions of Eq. (7) are valid.[9]

Figure 2 illustrates the frequency dependence and relative values of the reciprocals of the Baerwald asymptotic signal velocity, the Brillouin signal velocity, and the group velocity under the conditions of Eq. (7), and for an input signal at frequency ω. In order to get a feeling for the size of the reciprocal of the Brillouin velocity, which cannot be expressed in closed form, it may be noted that its maxima are at the points of intersection with the reciprocal group velocity; therefore, it is always smaller than the maxima of the latter.

Application to Ultrasonic Paramagnetic Resonance

A propagation medium consisting of a crystal containing paramagnetic impurities is not exactly equivalent to the model system of uncoupled oscillators in a gas or liquid, used in the theory, since the paramagnetic ions are coupled through dipolar and exchange forces. However, Jacobsen and Stevens[10] have shown that for the interaction of ultrasonics with a dilute system of paramagnetic ions, each of which has several resonant frequencies, ω_i,

$$k^2(\omega)=\frac{\omega^2}{c^2}\left[1+\sum_i \frac{A_i}{\delta^2+\omega_i^2-\omega^2-2i\omega\delta}\right]^{-1}, \tag{10}$$

where δ includes the line broadening effects mentioned above. For ω in the region of only one resonant frequency, ω_0, and using Eq. (7), Eq. (10) reduces to Eq. (4) with $A=-a^2$. Also, although the propagation medium is not a continuum, microwave frequencies are so low, compared with the cutoff frequency, that the normal dispersion in the crystal may be considered zero and c assumed independent of frequency. Thus, the results of velocity computations for plane ultrasonic waves propagating in a crystal containing a uniform distribution of paramagnetic ions, all having the same resonant frequency, will be identical to the results given above.

In Baerwald's calculation $k^2(\omega)$ is approximated by its value in the range $\omega\approx\omega_0$. In this case, and applying Eq. (7) again,

$$\begin{aligned}\alpha(\omega)&\approx\frac{\omega}{c}\left[1+\frac{a^2}{4\omega}\frac{\omega_0-\omega}{(\omega_0-\omega)^2+\delta^2}\right],\\ \beta(\omega)&\approx\frac{\omega}{c}\left[\frac{a^2}{4\omega}\frac{\delta}{(\omega_0-\omega)^2+\delta^2}\right],\end{aligned} \tag{11}$$

where, for ultrasonic paramagnetic resonance,

$$a^2=\frac{2\omega G^2|\langle|M|\rangle|^2 n}{\hbar\rho c^2}.$$

G is the spin-phonon coupling constant,[11] $\langle|M|\rangle$ is the matrix element of the relevant spin operator between the spin energy levels involved, ρ is the crystal density, and n is the population difference per cm^3 of the energy levels. In the usual nomenclature of paramagnetic resonance, $\delta\equiv T_2^{-1}$. Thus, $\beta(\omega)$ may be expressed as

$$\beta(\omega)=\frac{\pi G^2|\langle|M|\rangle|^2 n\omega g(\omega-\omega_0)}{2\hbar\rho c^3}, \tag{12}$$

where $g(\omega-\omega_0)$ is a normalized absorption line shape,

$$g(\omega-\omega_0)=\frac{T_2/\pi}{1+T_2^2(\omega-\omega_0)^2}. \tag{13}$$

The paramagnetic ions in MgO are located in Mg sites with cubic (octahedral) symmetry; however, due to small randomly distributed local departures from cubic symmetry, the spin energy levels are shifted

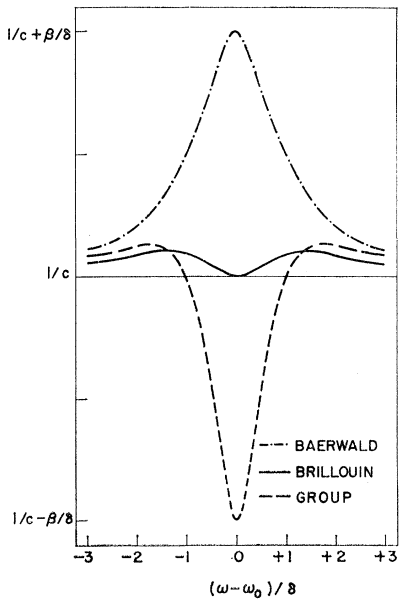

FIG. 2. Frequency dependences of the three velocities referred to in the text, under the conditions $\beta\ll\omega_0/c$, $\delta/\omega\ll 1$.

[8] M. A. Biot, Phys. Rev. **105**, 1129 (1957).
[9] See, for example, reference 4, pp. 119–123.
[10] E. H. Jacobsen and K. W. H. Stevens, Phys. Rev. (to be published).
[11] G values for Ni^{2+} and Fe^{2+} in MgO have been reported: N. S. Shiren, Bull. Am. Phys. Soc. **7**, 29 (1962).

slightly from their cubic field values, leading to inhomogeneously broadened magnetic resonance lines.[12,13] For each occupied point on the magnetic lattice, whose coordinates are x, y, z, there is a corresponding resonant frequency, $\omega_0(x,y,z)=\omega'$. Thus, $k^2(\omega)$ is a random function of position, and the ultrasonic wave in the crystal traverses randomly distributed regions having different resonant frequencies.

The problem we have to consider is similar to that of scattering of waves due to a randomly varying refractive index[14]; however, the present case is further complicated because the probability distribution of the refractive index is a function of the frequency of the primary wave. Also, our interest is not in amplitude or phase fluctuations but in the signal velocity obtained by evaluation of Eq. (3) in the random medium. Furthermore, it is important to note that we are not concerned with nonmagnetic causes (such as density fluctuations) of randomly varying refractive index since, as will be shown in Sec. III, the experiment is not sensitive to these. Our interest in the crystal inhomogeneities is only insofar as they are the source of inhomogeneous line broadening, and, therefore, give rise to a random spatial variation of resonant frequency.

We assume that the distribution of resonant frequencies, ω', is given by the function $h(\omega'-\omega_0)$, normalized so that

$$\int_0^\infty h(\omega'-\omega_0)d\omega'=1. \tag{14}$$

The observed magnetic resonance absorption is then the statistical mean formed by integrating the homogeneous line shape, Eq. (13), over the distribution of resonant frequencies.[15] In analogy with the homogeneous line shape, $g(\omega-\omega')$, we define δ^* such that the observed absorption line shape is normalized with a peak value $(\pi\delta^*)^{-1}$, at $\omega=\omega_0$. Thus for large inhomogeneous broadening, the line shape approaches $h(\omega-\omega_0)$, and

$$h(0)\approx 1/\pi\delta^*. \tag{15}$$

If the dimensional scale of the spatial inhomogeneities is small, so that the whole distribution of resonant frequencies is contained within regions small compared with the wavelength, then we can approximate $k^2(\omega,x,y,z)$ by its statistical average,

$$\langle k^2(\omega,x,y,z)\rangle_{\rm av}=\int_0^\infty k^2(\omega,\omega')h(\omega'-\omega_0)d\omega', \tag{16}$$

independent of x, y, z. If, furthermore, the conditions, Eq. (7), are valid for $\langle k^2(\omega)\rangle_{\rm av}$ (with δ^* substituted for δ), then in the integrand of Eq. (3) we substitute for $\alpha(\omega,x,y,z)$ and $\beta(\omega,x,y,z)$ their average values given, respectively, by

$$\langle\alpha(\omega)\rangle_{\rm av}\approx\int_0^\infty \alpha(\omega,\omega')h(\omega'-\omega_0)d\omega', \tag{17}$$

$$\langle\beta(\omega)\rangle_{\rm av}\approx\int_0^\infty \beta(\omega,\omega')h(\omega'-\omega_0)d\omega'. \tag{18}$$

Portis[15] has shown that the averaged absorption, Eq. (18), and the averaged dispersion, $[\langle\alpha(\omega)\rangle_{\rm av}-\omega/c]$, obey the Kramers-Kronig relationships; thus, if $\langle\beta(\omega)\rangle_{\rm av}$ is known $\langle\alpha(\omega)\rangle_{\rm av}$ may be computed from it. In general, the signal velocity will differ from that computed for a Lorentz absorption line shape. However, if $\langle\beta(\omega)\rangle_{\rm av}$ does exhibit a Lorentz shape then $\langle\alpha(\omega)\rangle_{\rm av}$ will have the form given in Eq. (11), and the group and signal velocities will have the shapes shown in Fig. 2, with abcissa, $(\omega-\omega_0)/\delta^*$.

When the scale of the inhomogeneities is large, so that the refractive index is slowly varying over distances of the order of several wavelengths, the above analysis is incorrect. However, in this case the problem may be treated by ray optics if the crystal dimensions (X,Y,Z) are still large compared with the scale of the inhomogeneities.

We approximate the plane wave, propagating in the x direction, by a ray bundle. For each ray the values of y, z are fixed and only variations of the parameters along x need be considered. Let $S(\omega,x,y,z)$ be the signal velocity in the neighborhood of the point (x,y,z) for an incident wave of frequency ω. Then the arrival time of the ray at X is

$$t(\omega)=\int_0^X [S(\omega,x,y,z)]^{-1}dx. \tag{19}$$

Since we have assumed the crystal dimensions to be large, the arrival time of the wave front at X approaches the statistical mean value,

$$\langle t(\omega)\rangle_{\rm av}\approx X\int_0^\infty [S(\omega,\omega')]^{-1}h(\omega'-\omega_0)d\omega'. \tag{20}$$

For the Baerwald asymptotic signal velocity, Eq. (9), the reduced arrival time is

$$[\langle t(\omega)\rangle_{\rm av}-t_c]_A\approx X\int_0^\infty [\beta(\omega,\omega')/\delta]h(\omega'-\omega_0)d\omega', \tag{21}$$

where $t_c=X/c$. In paramagnetic systems δ is the half-width of the homogeneously broadened "spin packets." It is independent of frequency for $\omega\gg\delta$, and may therefore be taken in front of the integral sign. Then

$$[\langle t(\omega)\rangle_{\rm av}-t_c]_A\approx X\langle\beta(\omega)\rangle_{\rm av}/\delta, \tag{22}$$

[12] J. W. Orton, P. Auzins, and J. E. Wertz, Phys. Rev. Letters **4**, 128 (1960).
[13] N. S. Shiren, Phys. Rev. Letters **6**, 168 (1961).
[14] L. A. Chernov, *Wave Propagation in a Random Medium* (McGraw-Hill Book Company, Inc., New York, 1960).
[15] A. M. Portis, Phys. Rev. **91**, 1071 (1953).

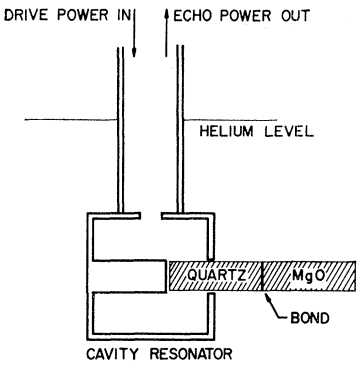

FIG. 3. Schematic diagram showing ultrasonic drive cavity and crystal arrangement.

where $\langle\beta(\omega)\rangle_{\rm av}$ is the observed absorption, Eq. (18), and is the same as that for the case of small scale inhomogeneities.

The arrival time appropriate to the Brillouin signal velocity in the presence of inhomogeneous broadening cannot be expressed in closed form, and must be computed numerically from Eq. (20). For large inhomogeneous broadening the respective arrival times are roughly proportional to the integrals over the velocity profiles shown in Fig. 2 (but including the tails which approach the same value). Performing the integrations we find for the ratio of the lower limit (Brillouin) reduced arrival time to the asymptotic value,

$$[\langle t(\omega)\rangle_{\rm av}-t_c]_L/[\langle t(\omega)\rangle_{\rm av}-t_c]_A\approx 0.32. \qquad (23)$$

III. EXPERIMENTAL METHOD

The attenuation and velocity of 9.5 Gc/sec ultrasonic pulses were measured using a pulse echo technique similar to that originally used by Jacobsen.[16] Figure 3 is a schematic diagram of the acoustic spin resonance "head" which is immersed in liquid He. Half-microsecond rf drive pulses were fed to the cavity resonator from an MA218 magnetron. Quartz transducers were bonded to MgO crystals having optically polished, parallel faces. Both quartz and MgO were 1–2 cm long and 3 mm in diameter. Only longitudinal waves propagating on the ⟨100⟩ axis of the MgO were used in making the measurements reported here. However, the effect has also been observed with longitudinal waves propagating on ⟨110⟩ and ⟨111⟩ axes, and with transverse waves on ⟨100⟩ axes.

The acoustic echo pulses were picked up in the cavity and detected by a superheterodyne receiver. The detected output was proportional to amplitude and therefore the observed pulses gave $|F(t,x)|$. Echoes were received from both the bonding surface and the far end of the MgO. The former provided a convenient fiducial mark (the first pulse in Fig. 1) for measuring the traversal times of the pulses through the MgO.

The velocity of longitudinal ultrasonic waves on the ⟨100⟩ axis of MgO was measured to be 9.25×10^5 cm/sec; thus, for frequencies ≈ 10 Gc/sec the crystal dimensions were very large compared with the wavelength. The measured absorptions, $\langle\beta\rangle_{\rm av}$, were of order unity and the largest line half-width observed was 0.7 Gc/sec, so the conditions, Eq. (7), were fulfilled even with inhomogeneous broadening.

The ions Ni^{2+} and Fe^{2+} were present in our MgO crystals in fractional concentrations of about 5 and 75 per 10^6 Mg ions, respectively. In addition, the crystals contained similar amounts of the paramagnetic ions Mn^{2+}, Fe^{3+}, and Cr^{3+}.

The ground states of Ni^{2+} and Fe^{2+} in octahedral environments both have effective spin $S=1$. In an external dc magnetic field H_0 there are, therefore, three Zeeman energy levels separated in frequency by $\gamma H_0/2\pi$.[17] Measurements were made on the $\Delta M=2$ transition of Ni^{2+}, and on both $\Delta M=1$ and $\Delta M=2$ transitions of Fe^{2+}. The line shapes were measured at a constant ultrasonic frequency by varying H_0. This method has the advantage that any nonmagnetic contributions to the absorption or dispersion were maintained constant during the run. The magnetic field was measured with a proton resonance gaussmeter.

The transition matrix element, $\langle|M|\rangle$, varies with the angle, θ, of the magnetic field with respect to the ⟨100⟩ propagation direction,[18] and the absorption varies as $(\cos\theta\sin\theta)^2$ for $\Delta M=1$ transitions, and as $\sin^4\theta$ for $\Delta M=2$ transitions. By adjustment of magnetic field angle, the ultrasonic-spin interaction could be made large enough to give a measurable velocity change, but was still small enough to provide a good signal-to-noise

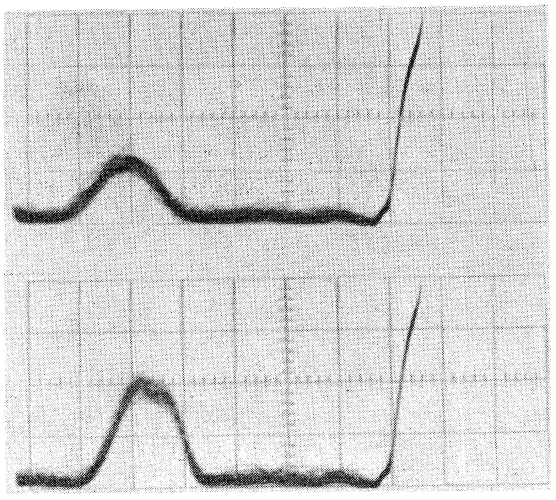

FIG. 4. Oscilloscope traces showing peak absorption and change in ultrasonic signal velocity due to interaction with Ni^{2+} $\Delta M=2$ resonance in MgO. Time increases from right to left. The second pulse has made one round trip through the MgO. Upper trace: ultrasonic frequency on resonance. Lower trace: ultrasonic frequency off resonance.

[16] E. H. Jacobsen, Phys. Rev. Letters **2**, 249 (1959).

[17] For Ni^{2+}, $\gamma/2\pi=3.09$ Mc/sec/Oe; and for Fe^{2+}, $\gamma/2\pi=4.80$ Mc/sec/Oe.

[18] N. S. Shiren and E. B. Tucker, Phys. Rev. Letters **6**, 105 (1961).

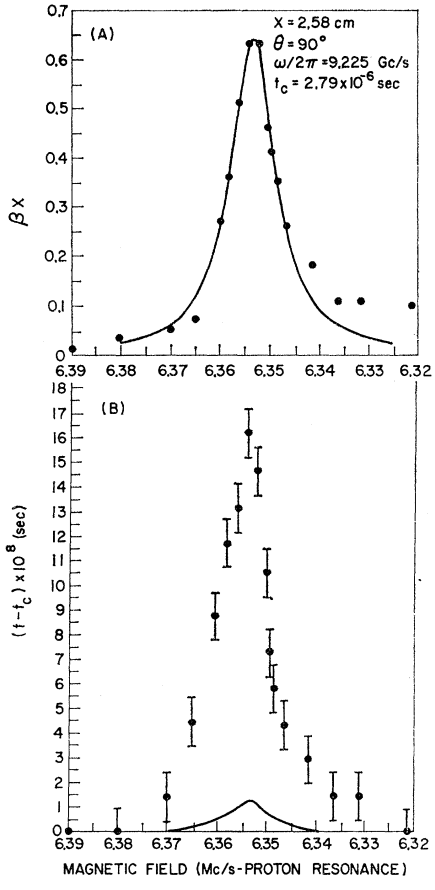

FIG. 5. A. Ni^{2+} $\Delta M=2$ absorption measurements vs magnetic field, and (solid line) Lorentz line shape fitted to the data. B. Ni^{2+} arrival time measurements vs magnetic field, and (solid line) asymptotic arrival time predicted from small scale theory.

ratio, and also to avoid extreme pulse distortion effects. It was necessary to maintain low power levels in order to avoid saturation effects, and the operating level was determined by turning down the power until no further change in absorption coefficient was observed.

Figure 4 shows the oscilloscope traces taken on the peak of the Ni^{2+} $\Delta M=2$ resonance and off resonance, and illustrates the magnitude of the effect under the conditions for which quantitative data were taken. Only the stationary part of the signal is seen since the forerunners have frequency components lying outside the detection bandwidth of 10 Mc/sec. Thus the signal was observed under the condition, used in the definitions of signal velocity, that the signal amplitude has reached its stationary value. Correspondingly, we found that time measurements made at any constant fraction of the peak pulse amplitude all gave the same value (within the measurement error) for the reduced arrival time, $(t-t_c)$, as a function of the input frequency ω. The attenuation was measured at the position of peak pulse amplitude and the measured value was taken as the best estimate of $\langle\beta(\omega)\rangle_{av}$. That is, in accordance with Eqs. (5) and (18), the stationary amplitude is

$$|F(t,x)|=|f(t)|e^{-\langle\beta(\omega)\rangle_{av}X},$$

where $f(t)$ is the input signal.

IV. RESULTS

Data taken on the Ni^{2+} and Fe^{2+} $\Delta M=2$ lines are presented in Figs. 5 and 6, respectively. In each case the upper figure (A) shows the measured absorption, $[\beta(\omega)X]$,[19] and the lower figure (B) shows the observed change in arrival time, $[t(\omega)-t_c]$. Both are plotted as functions of magnetic field, measured in units of the proton resonant frequency.[20] The asymmetric absorption line shapes are characteristic of these strain broadened $\Delta M=2$ transitions.[21] The total path length, X, represents one round trip in the MgO crystals.

Within the experimental errors, the observed field dependences of the signal velocities follow the absorption line shapes. This result is in qualitative agreement with the asymptotic signal velocity, Eqs. (9) and (22), for both large and small scale inhomogeneities. It is also in agreement with the Brillouin signal velocity if the theory for large scale inhomogeneities is applicable, and the inhomogeneous broadening is large ($\delta^*\gg\delta$). In the latter case the statistical average of the reduced arrival time will not exhibit the decrease in the region $\omega\approx\omega_0$, which is characteristic for a homogeneous line, and the arrival time profile will again follow the inhomogeneous absorption line shape.

Apart from the small asymmetry, the Ni^{2+} absorption is closely fitted by a Lorentz line shape (solid curve in Fig. 5A) with

$$\beta(\omega_0)X=0.64,$$

and a half-width at half-maximum,

$$H=1.29 \text{ Oe},$$

or

$$\delta^*/2\pi=7.97 \text{ Mc/sec}.$$

This provides an opportunity for a quantitative comparison with the theory for the case of small scale inhomogeneities, since then, according to the discussion following Eq. (18), if $\langle\beta(\omega)\rangle_{av}$ has a Lorentz shape, the asymptotic reduced arrival time should be

$$[\langle t(\omega)\rangle_{av}-t_c]_A{}^*=\langle\beta(\omega)\rangle_{av}X/\delta^*. \quad (24)$$

Using the experimental values given above, we then have for the predicted maximum change in arrival time

$$\beta(\omega)X/\delta^*=1.3\times10^{-8} \text{ sec}.$$

The corresponding magnetic field dependence is shown in Fig. 5(B) (solid curve). It is evident that the measured reduced arrival times are an order of magnitude

[19] When referring to experimental measurements, the averaging symbol will be dropped.
[20] For protons in water $\gamma/2\pi=4.25776$ kc/sec/Oe.
[21] W. Low and M. Weger, Phys. Rev. **118**, 1130 (1960).

larger, with a peak value

$$t(\omega_0)-t_c=1.6\times10^{-7}\text{ sec.}$$

Since the observed absorption, βX, is of order unity, the total path length lies in the region $X\approx x_{\text{crit}}$; therefore, the measured arrival times are expected, from theory, to be intermediate between the upper and lower limits established by the Baerwald and Brillouin calculations, respectively. An exact calculation of the theoretical arrival time appropriate to the experimental value of X (relative to x_{crit}) is beyond the scope of this paper. However, the theory for large scale inhomogeneities may be compared with experiment by using Eq. (22) to establish an upper limit and noting, from Eq. (23), that if the inhomogeneous broadening is large, the upper and lower limits differ by a factor approximately 3. Thus, the agreement of theory with experiment may be considered better than this factor if the true spin-packet half-width lies in the range

$$0.32\beta(\omega_0)X[t(\omega_0)-t_c]^{-1}<\delta<\beta(\omega_0)X[t(\omega_0)-t_c]^{-1}. \quad (25)$$

For Ni^{2+}, Eq. (25) yields

$$1.3\times10^6/\text{sec}<\delta<4.0\times10^6/\text{sec.}$$

The ratio, $\delta^*/\delta>10$, is consistent with the assumption of large inhomogeneous broadening.

The results of the Fe^{2+} $\Delta M=2$ measurements (Fig. 6) are similar. The observed arrival time curve closely follows the inhomogeneously broadened absorption line shape, but the measured values are again much larger than expected if the inhomogeneous linewidth, δ^*, is taken for δ.

An average value for δ^* may be computed according to Eq. (15), by normalizing the absorption curve, $h(\omega-\omega_0)$, and setting $h(0)=1/\pi\delta^*$. Taking ω_0 as the frequency for maximum absorption yields

$$\delta^*=2.96\times10^8/\text{sec.}$$

The measured peak absorption was

$$\beta(\omega_0)X=1.57,$$

and the observed, reduced arrival time was

$$t(\omega_0)-t_c=1.1\times10^{-7}\text{ sec.}$$

Since βX is again such that $X\approx x_{\text{crit}}$, the theory for large scale inhomogeneities, Eq. (22), requires that the spin-packet linewidth be

$$4.5\times10^6/\text{sec}<\delta<1.4\times10^7/\text{sec.}$$

Data taken on the Fe^{2+} $\Delta M=1$ transition also gave similar results. This line has an approximately Gaussian shape with a peak to peak absorption derivative width of 370 Oe. Thus,

$$\delta^*\approx4.5\times10^9/\text{sec.}$$

As in the case of the other transitions, the arrival time curve had the absorption line shape. The maximum increase in arrival time was

$$t(\omega_0)-t_c=1.0\times10^{-7}\text{ sec,}$$

for a peak absorption

$$\beta(\omega_0)X=0.64.$$

The homogeneous broadening required for agreement with the large scale theory is

$$2.0\times10^6/\text{sec}<\delta<6.4\times10^6/\text{sec.}$$

As stated earlier, these measurements were made at power levels sufficiently low to avoid saturation of the transitions. At higher power levels all three transitions exhibited a decrease (with increasing power) of the observed attenuation, but a much smaller concomitant change in the signal velocity. The photographs of Fig. 1 were made on the Fe^{2+} $\Delta M=1$ transition at high power levels, and at an angle such that $|\langle|M|\rangle|$ was large, in order to demonstrate a large velocity change without having the pulse completely disappear in the noise.

In Fig. 1, the observed absorption is 1.53; however, from the known G value and angular variation, the unsaturated absorption is calculated to be

$$\beta(\omega_0)X=5.2.$$

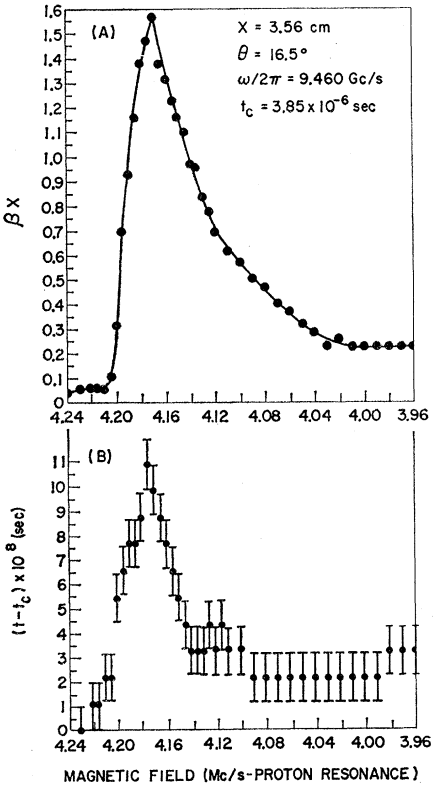

FIG. 6. (A). Fe^{2+} $\Delta M=2$ absorption measurements vs magnetic field. (B). Fe^{2+} $\Delta M=2$ arrival time measurements vs magnetic field.

The measured reduced arrival time was

$$t(\omega_0)-t_c=7.3\times10^{-7}\text{ sec.}$$

The ratio of this value to that of the low power measurement reported above is approximately equal to the ratio of the unsaturated absorption values. Thus, in the present case, although the absorption is saturated by a factor 3.5, the velocity remains practically unchanged.

V. DISCUSSION

From the form of the dispersion associated with an inhomogeneously broadened absorption line[15] it is easily shown that the resulting group velocity must be larger than c over some frequency range. Therefore our measured signal velocities cannot be in agreement with the group velocity.

We have shown, in the case of Ni^{2+}, that our measurements are not in agreement with theory if small scale inhomogeneities are assumed. For the Fe^{2+} lines the comparison of experiment with theory, under the small scale assumption, is less exact because the line shapes are not Lorentzian. However, the values of δ^*, computed in Sec. IV, should yield reasonable approximations to the correct theoretical arrival times. In Table I we have listed reduced arrival times, $[\langle t(\omega_0)\rangle_{\text{av}}-t_c]_A^*$, computed from the asymptotic formula, Eq. (24), on the basis of small scale inhomogeneities. It is clear that they are in violent disagreement with the measured values, also listed in Table I. In addition, the size of the discrepancy varies from one to three orders of magnitude over the three lines. This, in itself, strongly suggests that the lack of agreement cannot be attributed to failure of the theory of signal velocity, but must be due to the small scale assumption.

As was pointed out earlier, the experimental results are in qualitative agreement with the calculations of Brillouin and Baerwald, provided we assume large scale inhomogeneities and large inhomogeneous broadening. In order to make a quantitative comparison we have calculated spin-packet widths, δ_D, from the theory of dipolar broadening. These calculations are given in the Appendix, and in Table II we list the upper limits on δ_D, computed from Eqs. (28), (29), and (30). Also listed in the table are the values of δ^*, and the upper limits on δ (from Sec. III) required for theory and experiment to agree.

TABLE I. Observed reduced arrival times, $[t(\omega_0)-t_c]$, and upper limits, $[\langle t(\omega_0)\rangle_{\text{av}}-t_c]_A^*$, computed from theory assuming small-scale inhomogeneities. Units are 10^{-7} sec.

Line	$[t(\omega_0)-t_c]$	$[\langle t(\omega_0)\rangle_{\text{av}}-t_c]_A^*$
Ni^{2+} ($\Delta M=2$)	1.6	0.13
Fe^{2+} ($\Delta M=2$)	1.1	0.053
Fe^{2+} ($\Delta M=1$)	1.0	0.0016

TABLE II. Upper-limit spin-packet half-widths required for agreement of large-scale theory with experiment, those computed from dipolar broadening, and measured inhomogeneous half-widths.

Line	δ	δ_D	δ^*
Ni^{2+} ($\Delta M=2$)	4.0×10^6/sec	7.3×10^6/sec	5.1×10^7/sec
Fe^{2+} ($\Delta M=2$)	1.4×10^7/sec	1.7×10^7/sec	3.0×10^8/sec
Fe^{2+} ($\Delta M=1$)	6.4×10^6/sec	9.3×10^6/sec	4.5×10^9/sec

From Table II we note that (δ^*/δ_D) is large for all three transitions, so the assumption of large inhomogeneous broadening is valid. (However, as stated earlier, this assumption is not necessary to establish the required upper limit on δ.) In view of the approximations made in the calculation of dipolar broadening, in the derivation of our Eq. (21), and in the theory of signal velocity, the fact that the dipolar upper limits are larger by factors <2 than the required values of δ is considered satisfactory. As discussed in the Appendix, it is difficult to calculate δ_D accurately; however, referring to that discussion, it does not appear unreasonable that δ_D lies within the required range.

As an additional check on the theory we note again that for all three transitions $X\approx x_{\text{crit}}$, and that small differences in X produce very small variations in the reduced arrival times, since the total theoretical variation of the latter, from $X\ll x_{\text{crit}}$ to $X=\infty$, is only a factor 3. Thus, although we cannot ascertain exact values of δ, among the three transitions the relative values (which are not affected by whether upper or lower limits are taken) should be roughly in the same ratio as those of δ_D (also unaffected by which limit is taken). From Table II it is seen that the two sets of ratios agree within 50% or better.[22]

We now make some remarks regarding the relative saturation behavior of the absorption and velocity. This is similar to that observed for the magnetic resonance absorption and dispersion signals of inhomogeneously broadened lines.[23] However, the origins of the effects are probably not the same. In the present case, even for a homogeneous line, the integral of Eq. (3) is altered; the principal effects of saturation being to introduce two branch points above the real axis. Equation (3) is then no longer a proper solution of the wave equation and the theory, as presently constituted, cannot predict saturation effects.

[22] *Note added in proof.* Since the dipolar broadening is proportional to the paramagnetic ion concentration, it was suggested by N. Bloembergen that a better test of the large-scale theory was to repeat the measurement in a crystal having a different concentration. This measurement has been made and reported at the First International Conference on Paramagnetic Resonance, Jerusalem, Israel, July 16–20, 1962. The results are in agreement with the conclusions of this paper.

[23] See reference 15, Sec. VI, but note that the susceptibility expression used there is proportional to $[(\omega_0-\omega)+i\delta]^{-1}$, while ours is proportional to $[(\omega_0-\omega)-i\delta]^{-1}$.

VI. CONCLUSION

We have found that the experimental results confirm the theory of signal velocity in a region of resonant absorption as calculated by Brillouin and Baerwald, provided we assume that the spatial variation of resonant frequencies is slow over distances of the order of the ultrasonic wavelength (10^{-4} cm). It was also found that if the variation is assumed rapid, the discrepancy between theory and experiment is so large as to make even the qualitative features of the theory incorrect.

It, therefore, seems likely that the theory of signal velocity is correct, and that ultrasonic velocity measurements provide a technique for the determination of the scale of inhomogeneities on a magnetic lattice. Furthermore, they also may be used as a technique for measuring spin packet widths in the presence of inhomogeneous broadening.

ACKNOWLEDGMENTS

It is a pleasure to acknowledge the invaluable assistance of T. G. Kazyaka. I also wish to thank Dr. G. J. Lasher and Dr. A. H. Nethercot for reading the manuscript and making several helpful suggestions.

APPENDIX

Calculation of Spin-Packet Linewidths

Formulas for the moments of spin-packet line shapes observed in ultrasonic paramagnetic resonance have been derived by Loudon.[24] Since the fractional concentration of paramagnetic ions in our crystals was of order 10^{-5}, contributions to the linewidth due to exchange may be neglected. In addition, it is known from paramagnetic resonance data that, for the resonances of interest in this paper, the deviations from cubic symmetry of the local environment are very small[20,25]; therefore, the neighboring Mg sites are not occupied by other paramagnetic ions.

Kittel and Abrahams[26] have shown that for fractional concentrations smaller than 10^{-2} the spin-packet line, due to dipolar broadening only, has a cutoff Lorentz shape. The cutoff frequencies depend on the ratio of the fourth to second moments. Using this formulation we have extended Loudon's results to the case of magnetically dilute salts. The dipolar broadening of phonon-induced $\Delta M=1$ transitions due to a single magnetic ingredient is found to be

$$\delta_D=(\pi/4\sqrt{2})(fA/\hbar)(S^2+S)^{1/2}\times[1.79-0.572(S^2+S)^{-1}]^{-1/2}; \quad (26)$$

and for phonon-induced $\Delta M=2$ transitions

$$\delta_D=(\pi/3\sqrt{6})(fA/\hbar)(S^2+S)^{1/2}\times[0.811-0.408(S^2+S)^{-1}]^{-1/2}. \quad (27)$$

In the above formulas, f is the fractional magnetic concentration, S is the spin, and

$$A=(\sum_k{}'B_{jk}{}^2)^{3/2}/(\sum_k{}'B_{jk}{}^4)^{1/2}.$$

B_{jk} is given in Eq. (2) of reference 25, and the summations are over sites k ($k\neq j$) on the magnetic lattice.

Equations (26) and (27) apply to the dipolar broadening due to like spins only. This is appropriate for the Fe^{2+} $\Delta M=2$ line. However, because of the low concentration of Ni^{2+}, dipolar broadening due to the presence of other magnetic ions dominates over that due to Ni^{2+} alone. Similar considerations apply to the Fe^{2+} $\Delta M=1$ line for which the inhomogeneous broadening is so large that most of the Fe^{2+} ions lie outside the homogeneous width associated with any other Fe^{2+} ion.

The dipole-dipole interaction between unlike spins is actually a source of inhomogeneous broadening and should not be included in a calculation of the homogeneous linewidth. However, the resulting distribution of resonant frequencies will be small compared with the observed distribution which is due to deviations from cubic symmetry; and since in our crystals the number of magnetic ions in a volume of order λ^3 is about 10^6, we expect the whole distribution of resonant frequencies due to dipolar broadening to be contained within regions small compared with the wavelength. Thus, these inhomogeneities fall under the small scale assumption and should properly be included in the line width which appears in the velocity formulas.

There is no available formulation of the broadening effect of other magnetic ingredients on ultrasonic paramagnetic absorption lines. However, as noted by Van Vleck,[27] the contribution of unlike spins is smaller by a factor 2/3 than that of like spins. We therefore treat the Fe^{2+} $\Delta M=1$ line and the Ni^{2+} $\Delta M=2$ line by taking 2/3 of the values computed from Eqs. (26) and (27), respectively, with f and B_{jk} referred to the unlike spins. For the latter we take Fe^{2+} since it had the largest concentration and highest γ of any of the ions present.

As mentioned above, nearby M_g sites are not occupied by magnetic ions; but since we have no knowledge as to how far from any given paramagnetic ion the sites remain unoccupied, it is difficult to evaluate δ_D accurately. However, we can compute an upper limit by carrying out the summations over all sites k ($k\neq j$) on the magnetic lattice. Calculations made by leaving out first, second, and third nearest neighbors yielded values of δ_D which were smaller than the upper limits by a factor 2.7.

The upper limit on δ_D computed from Eq. (27), for the Fe^{2+} $\Delta M=2$ transition is

$$\delta_D=9.06NB, \quad (28)$$

where N is the concentration of Fe^{2+} and $B=\gamma^2\hbar$. From

[24] R. Loudon, Phys. Rev. **119**, 919 (1960).
[25] W. Low, Phys. Rev. **109**, 247 (1958).
[26] C. Kittel and E. Abrahams, Phys. Rev. **90**, 238 (1953).
[27] J. H. Van Vleck, Phys. Rev. **74**, 1168 (1948).

the discussion above and Eq. (26), the upper limit for the Fe^{2+} $\Delta M=1$ line is

$$\delta_D \approx \tfrac{2}{3}[7.32NB]; \quad (29)$$

and for the Ni^{2+} $\Delta M=2$ line,

$$\delta_D \approx \tfrac{2}{3}[9.06NB']; \quad (30)$$

where $B'=\gamma\gamma'/\hbar$. Here, γ refers to Ni^{2+} and γ' refers to Fe^{2+}.

The Fe^{2+} concentration in the crystals used was $2.0\times10^{18}/cm^3$. With this value and the γ, γ' given in reference 17, Eqs. (28), (29), and (30) yield the δ_D listed in Table II.

PHYSICAL REVIEW VOLUME 128, NUMBER 5 DECEMBER 1, 1962

Electron Drift Mobility in Silver Chloride*

R. Van Heyningen
Research Laboratories, Eastman Kodak Company, Rochester, New York
(Received July 30, 1962)

The drift mobility of electrons in silver chloride has been measured in the temperature range 70 to 350°K. In selected crystals, multiple trapping effects are not important, and the data represent the microscopic mobility. The experimental results are compared with existing theories of mobility in polar materials. It is suggested that the microscopic mobility is determined by the interaction of longitudinal optical phonons with polarons which have a temperature-dependent mass, and a temperature-dependent coupling between the electron and the lattice. The effect of multiple trapping at lower temperatures is shown, and the results are analyzed in terms of the concentration and energy depth of a single set of shallow trapping states.

I. INTRODUCTION

MEASUREMENTS of the drift and Hall mobilities of electrons in silver chloride have been reported by several authors.[1–4] The greatest success in fitting existing theories of electron mobility in polar materials[5–8] to the silver chloride data has been realized in a temperature range appreciably below the Debye temperature. The comparison of theory and experiment at higher temperatures, however, has been more uncertain because of the lack of sufficiently precise data in the temperature range above and including the Debye temperature.

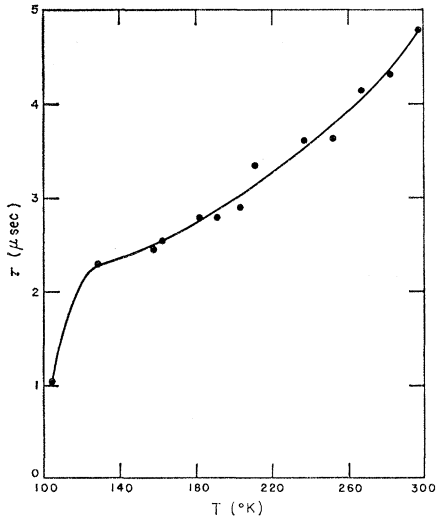

FIG. 1. Electron lifetime τ as a function of temperature in oxygen-doped AgCl, Sample C98–8.

The primary purpose of the present work was to clarify the experimental situation at higher temperatures, and thus provide a better check of available theories and for future theoretical work that may be more applicable to the case of silver chloride. Reproducible electron-mobility data, based on transit-time measurements, were obtained for a number of samples in the temperature range from 70 to 350°K. It was found that the available theories do not adequately describe the results.

II. EXPERIMENTAL

A. Electron Lifetime

Silver chloride is a wide bandgap photoconductor, and would, therefore, be an insulator in the dark were it not for its relatively large ionic conductivity. Impurity doping and mechanical strain affect the electronic as well as the ionic properties, and although these effects are not understood in detail, it is possible to prepare samples that have relatively long electron-trapping lifetimes (hereafter referred to simply as

* Communication No. 2311 from the Kodak Research Laboratories.

[1] J. R. Haynes and W. Shockley, Phys. Rev. **82**, 935 (1951).
[2] F. C. Brown and F. E. Dart, Phys. Rev. **108**, 281 (1957).
[3] K. Kobayashi and F. C. Brown, Phys. Rev. **113**, 508 (1959).
[4] L. Chollet and J. Rossel, Helv. Phys. Acta **33**, 627 (1960).
[5] D. Sowarth and E. Sondheimer, Proc. Roy. Soc. (London) **A219**, 53 (1953).
[6] R. L. Petritz and W. Scanlon, Phys. Rev. **97**, 1620 (1955).
[7] F. Low and D. Pines, Phys. Rev. **98**, 414 (1955).
[8] T. D. Schultz, Phys. Rev. **116**, 526 (1959).

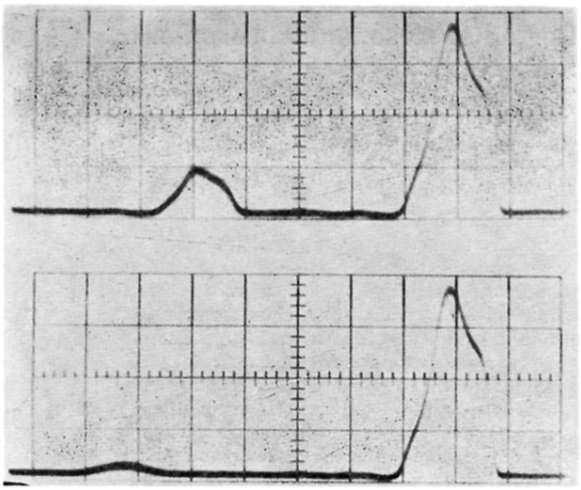

FIG. 1. Oscilloscope traces showing change in ultrasonic signal velocity due to interaction with Fe^{2+} spin resonance in MgO. Time increases from right to left. The first pulse is a bond echo and has traveled through the quartz transducer only. The second pulse has made one round trip in the MgO. Upper trace: ultrasonic frequency off resonance. Lower trace: ultrasonic frequency on resonance.

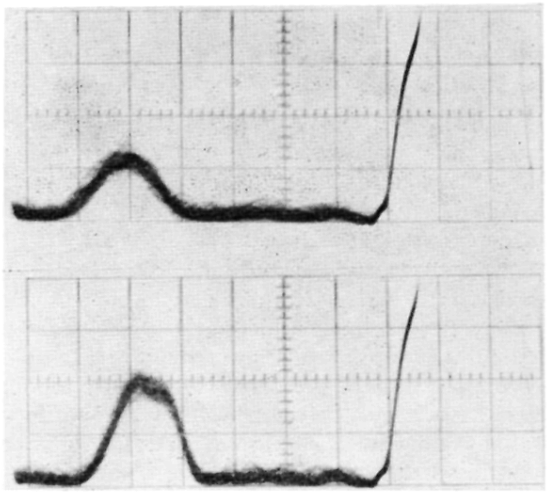

FIG. 4. Oscilloscope traces showing peak absorption and change in ultrasonic signal velocity due to interaction with Ni^{2+} $\Delta M=2$ resonance in MgO. Time increases from right to left. The second pulse has made one round trip through the MgO. Upper trace: ultrasonic frequency on resonance. Lower trace: ultrasonic frequency off resonance.